Crystal Structure and Stereoselective Solid-State Photodimerization of 1-(9-Anthryl)alkyl Acetates

Yukie Mori,* Yumiko Horikoshi, and Koko Maeda

Department of Chemistry, Faculty of Science, Ochanomizu University, Otsuka, Bunkyo-ku, Tokyo 112

(Received January 18, 1996)

X-Ray structure analyses of 1-(9-anthryl)alkyl acetates [AnCH(OAc)R; An=9-anthryl, R=Me (**1a**), Et (**1b**), *i*-Pr (**1c**), *t*-Bu (**1d**), CF_3 (**1e**)] indicated that these molecules adopted similar conformations in which the bond connecting the chiral carbon and the substituent was oriented almost perpendicular to the anthracene plane. In the crystals of **1b**—**1e** two adjacent anthracenes related by an inversion center was stacked with a short interplane distance (3.5—3.6 Å), which was favorable for the formation of the meso head-to-tail dimer. Photolysis of crystals of **1b**, **1c**, and **1e** afforded *meso*-dimers in almost 100% yield, while **1d** was photostable. The quantum yield of dimerization for **1b** (0.16) was higher than that in solution. Although the dimerization did not proceed in single crystal-to-single crystal fashion, the observed high selectivity suggested that the reaction took place between the π-stacking pair even when the crystalline lattice of the monomer was destroyed. Irradiation of **1a**—**1e** in benzene solution gave *meso*- and *dl*-head-to-tail dimers in a ratio of 1 : 1. The quantum yield of dimerization decreased with increase in the size of the substituent.

Solid-state photodimerization of anthracenes is a well-known reaction and the regioselectivity of head-to-tail (h–t) vs. head-to-head (h–h) dimers has been discussed for a long time in terms of violations of the topochemical rule.[1] The β type crystals of 9-cyanoanthracene and 9-anthracenecarboxyaldehyde exclusively yield the h–t dimers although the molecules are stacked with a h–h mutual orientation.[2] Craig and Sarti-Fantoni suggested in these crystals the dimerization took place at defects and/or surfaces, not in the bulk of the crystal.[2] Recently, Kaupp reported that the non-topochemical dimerization of these anthracenes can be explained by phase transformation with molecular transports, by means of the technique of atomic force microscopy.[3]

The way how the lattice constraint of the reactant crystal controls the reaction pathways is not so simple as to be fully explained by the topochemical rules. To answer this question is essential for investigation of dynamic aspects of solid-state reactions and design of a tailor-made crystal for a desired reaction. As far as the regioselectivity of h–t vs. h–h is concerned, the h–h dimer may be thermally labile and furthermore, steric and/or electrostatic repulsions are more severe in the transition state leading to the h–h dimer. On the other hand, an attractive interaction such as hydrogen bonding between the substituents can stabilize the h–h association, as was reported for *N*-(9-anthryl)methylacetamide.[4] If electronic or steric factors significantly affect the ratio of competing pathways, effects of the reaction medium may be obscured. To investigate how the crystal packing influences the selectivity and reactivity in the photodimerization, an ideal system must satisfy the conditions that the structure of the photoproduct indicates mutual location and orientation of the monomers in the reactant and that the competing dimerization processes take place with almost the same efficiency in the absence of constraint of the crystal lattice. Anthracenes having a chiral substituent in the 9-position can give two diastereomeric h–t dimers (*meso*- and *dl*-forms) with almost the same thermal stability, affording a suitable system from this viewpoint. In this study, photodimerization of a series of 1-(9-anthryl)alkyl acetates **1a**—**1e** has been investigated both in the solid state and in solution to discuss what factors control the reactivity and selectivity in the dimerization processes (Scheme 1). The dynamic aspect of

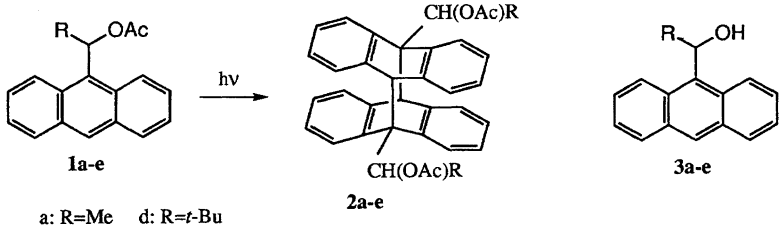

1a-e **2a-e** **3a-e**

a: R=Me d: R=*t*-Bu
b: R=Et e: R=CF_3
c: R=*i*-Pr

Scheme 1.

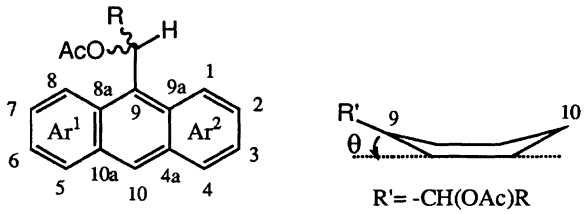

Fig. 1. Definition of planes and dihedral angles.

the solid-state reaction is also discussed based on the results of photochemistry and X-ray diffraction experiments.

Results and Discussion

X-Ray Structure Analysis. Table 1 summarizes selected structural parameters of **1a**—**1e**. In the crystal these molecules adopt similar conformations to each other, in which the acetoxyl group is inclined by 40—58° from the anthracene plane and the C_9–C_α–O–C(=O) angle is close to 90°. The torsion angle of C_{9a}–C_9–C_α–C_β tends to increase with the size of the substituent, although the correlation was not distinct. For **3e** it was reported that the C_α–CF_3 bond was almost perpendicular to the anthracene ring (ϕC_{8a}–C_9–C_α–$C_\beta = 93°$).[5] As for deviation from planarity of the anthracene, two dihedral angles were defined as in Fig. 1. As seen in Table 1, even in **1d** the angles were much smaller than those of 9-(1-hydroxy-1-methylethyl)anthracene ($Ar^1/Ar^2 = 15.3°$, $\theta = 11.5°$ [6]) and a little larger than those of 9-methoxyanthracene (4.6 and 1.4° [6]).

Table 1. Selective Structural Parameters

Compound	**1a**	**1b**	**1c**	**1d**	**1e**
Dihedral angle/°					
Two aryls (Ar^1/Ar^2)[a]	6.2	3.4	1.5	5.0	2.2
Folding angle (θ)[b]	2.2	0.4	0.3	3.2	0.9
Torsion angles/°					
C_{9a}–C_9–C_α–O	58.0	43.7	56.5	40.9	40.0
C_{9a}–C_9–C_α–C_β	−62.9	−76.5	−67.4	−83.0	−81.8
C_9–C_α–O–C(=O)	89.6	79.6	86.6	78.8	104.9
Interplane distance/Å	—	3.59	3.48	3.58	3.54
$C_9 \cdots C_{10'}$ distance/Å	—	4.01	3.80	4.17	3.85

a) Between the least-squares planes of C_1, C_2, C_3, C_4, C_{4a}, and C_{9a} and of C_5, C_6, C_7, C_8, C_{8a}, and C_{10a}. b) Between the least-squares plane of C_{9a}, C_{4a}, C_{10a}, and C_{8a} and the plane consisting of C_{9a}, C_9, and C_{8a}.

Possible directional forces[7] deciding crystal packing of **1a**—**1e** are face-to-face stacking of anthracenes, CH$\cdots\pi$, C–H$\cdots$O interactions, and dipole–dipole interaction of ester moieties. Racemic **1a**—**1e** were crystallized in a centrosymmetric space group, that is, spontaneous resolution did not take place. Any two crystals were not isomorphic, but in **1b**—**1e** a common characteristic packing was observed. Figure 2(a) shows the crystal structure of **1c** as a representative. Two adjacent anthracenes related by an inversion center were stacked with a short interplane distance, indicating that face-to-face stacking of anthracenes is the dominant intermolec-

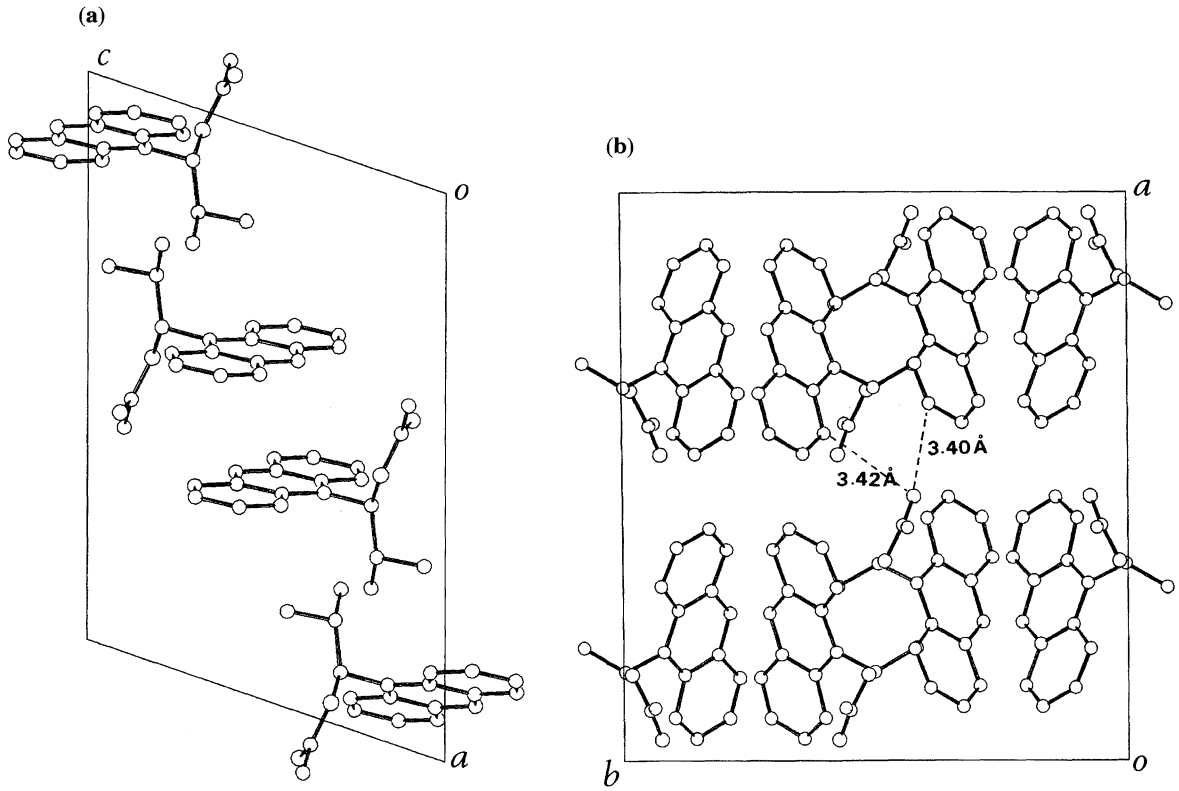

Fig. 2. (a) Crystal structure of **1c** viewed along the *b* axis. (b) Crystal structure of **1a** viewed along the *c* axis. The broken lines indicate short C–H$\cdots$O contacts. In both figures the H-atoms are omitted for clarity.

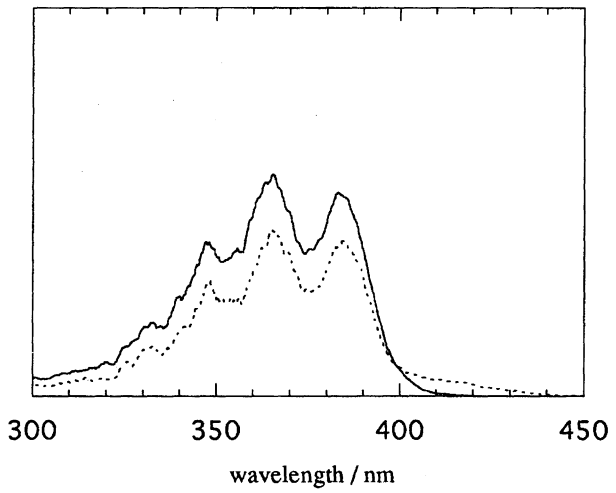

Fig. 3. Diffuse reflectance spectra. —: **1a**. - - -: **1c**

ular interaction in these crystals. The two anthracenes were shifted along the long and/or the short axis to some extent depending on the substituent, and therefore the interatomic distance of $C_9 \cdots C_{10'}$, where a new bond would be formed on dimerization, were somewhat different from each other. In **1c** the most effective overlap was attained and the distance was the shortest (Table 1). This type of molecular packing seems favorable to formation of the meso h–t dimer. In the crystal of **1a** such a π–π stacking pattern was not observed, but instead two short C–H···O(=C) contacts with the C···O distances of 3.40 and 3.42 Å were observed (Fig. 2(b)).

Electronic Spectra in the Solid State. Diffuse reflectance spectra of **1a** and **1c** in the powdery solid state showed a structured band in the region of 320—400 nm (Fig. 3), which was similar to the absorption spectrum recorded in a benzene solution. In the case of **1c** a broad band extending to 440 nm was observed, suggesting existence of interaction between the adjacent anthracenes. **1b** and **1e** showed a similar spectrum with a tailing around 430 nm, although the intensity was much weaker than that of **1c**. Figure 4 shows fluorescence spectra of **1a** and **1c** recorded in the powdery solid state at room temperature. The spectrum of **1a** was typical for fluorescence of the anthracene chromophore with resolved structure and a small Stokes shift, while **1c** showed a red-shifted broad emission the intensity of which was much weaker than that of **1a**. The spectral features observed for **1c** indicates significant intermolecular

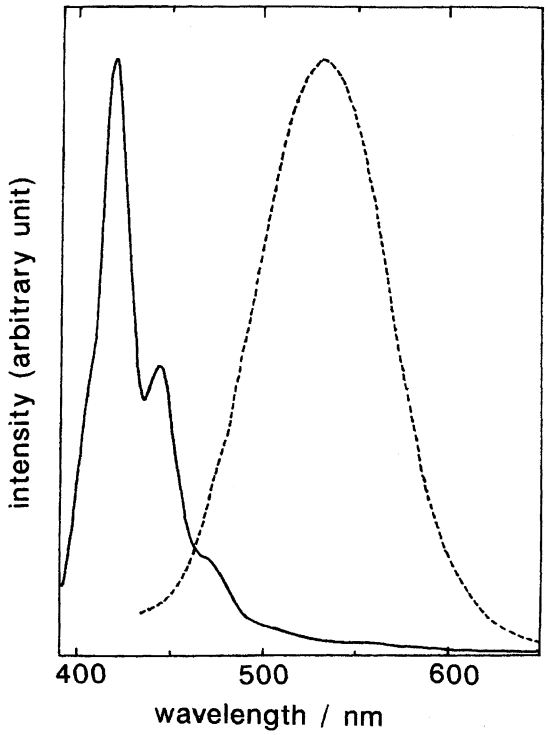

Fig. 4. Fluorescence spectra in the solid state. —: **1a** excited at 375 nm. - - -: **1c** excited at 390 nm.

interaction, which can be explained by a large overlap of the π system between two adjacent anthracenes in the crystal. A similar excimer-type fluorescence was reported for anthroate esters in the solid state.[8]

Solid-State Photodimerization. Solid-state photolysis was done in KBr pellets and progress of the reaction was monitored by a difference IR spectrum. After irradiation the reaction mixture was extracted and the ^{1}H NMR spectra were recorded. As is shown in Table 2, in the cases of **1b**, **1c**, and **1e**, dimerization proceeded smoothly and complete conversion was attained in 2 h. The structure of the dimer obtained from **1e** was found to be *meso*-**2e** because its IR and NMR spectra were clearly different from those of (*S*,*S*)-**2e**, which was formed from (*S*)-**1e**, **1b** and **1c** were also proved to give **2b** and **2c** as a single isomer respectively, based on a comparison of the NMR spectra with that of the dimer(s) formed in benzene solution. Considering from the crystal structure and analogy with dimerization of **1e**, the obtained dimer was assigned to the *meso*-form. When the powdered

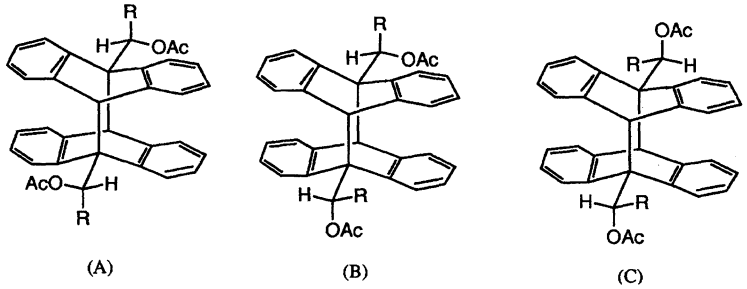

Fig. 5. Possible conformers for *meso*-**2c**.

Table 2. Yield and Diastereomer Ratio of Dimers Obtained on Solid-State Photolysis

Compd	Irr. time/h	Yield of **2**/%	d.e.
1a	53	14	0
1b	2	>97	>97
1c	2	>97	>97
1d	24	0	—
1e	2	>97	>97
(*S*)-**1e**	2	53	100[a]

a) (*S*,*S*)-**2e** was formed.

Table 3. Quantum Yields of Fluorescence and Dimerization at 365 nm in Benzene

Compd	Φ_f	Φ_{dim}
1a	0.44	1.9×10^{-2}
1b	0.43	1.5×10^{-2}
1c	0.43	3.3×10^{-3}
1d	0.51	$< 3 \times 10^{-4}$
1e	0.60	1.5×10^{-2}

Table 4. Coalescence Temperature and Activation Free Energy for Rotation around the C_9–C_α Bond

Compd	Solv.	$\delta_{1-H,8-H}$	(T/K)[a]	T_c/K	$\Delta G^{\neq}$/kcal mol^{-1} [b]
1a	CD_2Cl_2	8.31, 8.70	(163)	251	11.7
1b	CD_2Cl_2	8.39, 8.71	(233)	278	13.1
1c	$CDCl_3$	8.56, 8.74	(263)	313	15.2
1d	$CDCl_3$	8.53, 8.88	(298)	>323	>15.2
1e	$CDCl_3$	8.35, 8.73	(263)	>323	—

a) Under slow exchange condition. b) At T_c.

solid sample of **1b**, **1c**, and **1e** was irradiated between two Pyrex® plates under vacuum for larger-scale experiments, the same selectivity was observed as with KBr pellets. #

In the ^{1}H NMR spectrum of **2c** four signals assigned to C_α–H were observed, suggesting that three rotational isomers (Fig. 5) exist in a ratio of about 4 : 4 : 1. These isomers could not be separated on TLC and the ratio measured by NMR did not change after recrystallization. Assuming that the reaction pathway with minimal molecular motion proceeded during dimerization, **2c** formed in the crystal of **1c** should exist as the isomer (A) in which the isopropyl group lies antiperiplanar to the C_9–$C_{10'}$ bond. These facts suggested that the rotational isomers were in an equilibrium in solution. The same type of rotational isomerism was reported for the dimer of 9-(1-hydroxyl-1-methylethyl)anthracene, and each isomer was separated by chromatography.[6]

It is noteworthy that **1b**, **1c**, and **1e** exclusively gave the meso dimer even at complete conversion. The possibility that the selectivity might reflect the difference in stability between the two diastereomeric dimers or the transition states can be ruled out, because in benzene solution both *meso*- and *dl*-dimers were obtained in a 1 : 1 ratio (vide infra). If the reaction proceeded in single crystal-to-single crystal fashion, stereospecific dimerization would be obvious. To examine the possibility that the original crystal lattice of the monomer was retained during dimerization, the powdery solid sample of **1b** was photolyzed (> 330 nm) and the X-ray diffraction pattern was recorded at appropriate intervals. The peaks of **1b** were broadened at 30% conversion and completely disappeared at 90% conversion. When a single crystal of **1b** was also irradiated by much weaker, longer-wavelength light (> 380 nm), which is a suitable condition for crystalline state reactions,[9] the crystal gradually became opaque. These results indicate that the crystalline lattice of **1b** was not retained during dimerization. Recently in some solid-state reactions, long-range molecular transports were observed by Kaupp by atomic force microscopy.[3] In this case, if large-scale molecular transports took place during photoreaction, the well-ordered molecular packing of the monomer would be broken, and as a result two monomers which did not align in a suitable fashion for dimerization in the original crystal might dimerize. The observed high selectivity of the reaction suggested that each molecule reacted with the partner which had been destined for dimerization on crystallization. It is likely that in the crystals of **1b**, **1c**, and **1e** each molecule probably interacts with the π-stacking partner more strongly than with other neighboring molecules, which is consistent with the above assumption.

In spite of a similar crystal packing to photoreactive **1b**, **1d** was photostable; no variation in IR spectrum was detected after irradiation for 24 h. The separation of the potential reacting sites was somewhat larger than that in **1b**, but the distance was still less than 4.2 Å, which is the criterion proposed for dimerization of olefins by Schmidt.[10] The quantum yield for dimerization of **1c** (0.022) was lower in comparison with **1b** (0.16), although the $C_9 \cdots C_{10'}$ distance of **1c** was shorter than that of **1b**. The observed photochemical behavior of **1c** and **1d** suggested that the reactivity for photodimerization should be controlled by not only the $C_9 \cdots C_{10'}$ distance but also by other factors such as size and shape of the reaction cavity and intrinsic photoreactivity of the monomer.

During photolysis of **1a** no significant difference was observed in the IR spectrum in 2 h. When irradiated for a much longer period, however, **2a** was formed in a low yield as a 1 : 1 diastereomeric mixture. The much lower reactivity of **1a** in comparison with **1b**, **1c**, and **1e** can be explained by molecular packing in the crystal. From inspection of intermolecular distances, possible candidates for dimerization are a molecule related by a two-fold screw axis (to give *dl*-**2a**) and one related by a *c*-glide plane (to give *meso*-**2a**), but in both cases large molecular motion (about 6 Å) is necessary for the bond formation. The chiral crystal of **1e** gave (*S*,*S*)-**2e** in a relatively high yield (Table 2). A similar molecular packing to racemic **1e** may be attained, forming a pseudo-centrosymmetric pair with π–π stacking, but no single crystal of (*S*)-**1e** suitable for X-ray study was obtained.

Photodimerization in Solution. The absorption and fluorescence spectra of **1a**—**1e** showed a well-resolved structure typical for non-conjugated anthracenes and no anomalous

#In the presence of oxygen, a small amount of anthraquinone was also formed.

feature was observed. The quantum yield for fluorescence was not influenced by the bulkiness of the alkyl substituent (Table 3). These facts suggested that the perturbation of the electronic structure in the π system by the substituent should be negligible, as was expected based on the small deviation from planarity (Table 1).

When a solution of **1a**—**1e** in C_6D_6 was irradiated under vacuum at room temperature, the ^{1}H NMR signals assignable to the h–t dimers were detected. In the cases of **1a**—**1c** and **1e**, the corresponding dimers **2a**—**2c** and **2e** were isolated as the sole product, respectively. It was reported that (9-anthryl)methyl acetate gave h–h and h–t dimers in a ratio of 1 : 4 on irradiation in CH_2Cl_2.[11] In these cases no h–h dimer was detected, probably due to more severe steric repulsion between the substituents. On the photolysis of **1d**, ^{1}H NMR signals at $\delta = 4.5$ (10-H and 10′-H) and 2.15, 2.17 (COMe) indicated formation of **2d**, but it was not isolated because of thermal cycloreversion to give the starting monomer. As for the stereoselectivity, all the dimers obtained were a 1 : 1 mixture of *meso*- and *dl*-forms. In the ^{1}H NMR spectrum of the dimers recorded in C_6D_6 the singlet signals assigned to the acetoxyl protons of the diastereomers were separately observed. In the cases of **2a** and **2c** the ^{1}H NMR signals of C_α–H observed in $CDCl_3$ were also useful for measurement of the diastereomer ratio. In solution the excited molecule will encounter a homochiral molecule or an antipode with the identical probability, and therefore the lack of stereoselectivity indicates that the ratios of dimer formation vs. deactivation from the encounter complex are the same in both cases.

As is seen in Table 3, the dimerization efficiency decreased with increases in the size of the substituent at the 9-position. It is expected that the bulkiness of the substituent will be reflected in the energy barrier to rotation around the C_9–C_α bond. Indeed, the ^{1}H NMR spectra of **1b** and **1c** showed broad signals assigned to 1-H and 8-H at room temperature. The coalescence temperature T_c and the activation free energy at T_c were measured and listed in Table 4. In the case of **1d**, the 1-H and 8-H signals were separately observed as sharp doublets even at 298 K. The $\Delta G^{\neq}$ values of **1a**, **1c**, and **1e** were higher than those of the corresponding alcohols (11.0 at 245 K, 14.0 at 306 K and 14.5 at 320 K for **3a**, **3c**, and **3e**, respectively[12]). The rotational energy barrier of **3d** was reported to be 22.2 kcal mol^{-1} at 320 K, and probably **1d** has a higher barrier. In the stable conformation of the monomer the large substituent is almost perpendicular to the anthracene ring (Table 1). On dimerization the torsion angle of C_{9a}–C_9–C_α–C_β is reduced, which will cause more severe steric repulsion between the substituent and protons at the 1- and 8-positions. The substituent effect on the photoreactivity in solution is likely due to destabilization of the dimer by steric hindrance. The lack of solid-state photoreactivity of **1d** might be due to instability of **2d**.

Experimental

UV spectra were measured on a Shimadzu UV2200 spectrophotometer. Diffuse reflectance spectra of the sample diluted with $BaSO_4$ were recorded on a Shimadzu UV3100-PC using $BaSO_4$ as a reference. Fluorescence spectra were taken on a Shimadzu RF510 fluorophotometer connected with a personal computer through an A/D converter (Nippon Filcon Co., JJ-Joker J-1). The fluorescence quantum yields were measured with quinine sulfate in 0.5 M (1 M=1 mol dm^{-3}) H_2SO_4 as the standard. IR spectra were recorded on a Shimadzu FTIR-4100 spectrometer as a KBr disk. ^{1}H and ^{13}C NMR spectra were taken on a JEOL GSX270 or GSX400 spectrometer with tetramethylsilane or the residual proton of the solvent as internal standards. J values are given in Hz. Mps were obtained on a Yanaco micro apparatus and are uncorrected. X-Ray powder diffraction patterns were recorded with Cu $K\alpha$ radiation. The 2θ range of 10—50° was scanned with the scan speed of 2° min^{-1}. All the solvents used for spectrometry and photoreaction were of spectroscopic grade. Irradiation was done by a 400 W high-pressure mercury lamp through a 1 M aqueous potassium nitrate filter solution ($\lambda > 330$ nm) at about 25 °C using a merry-go-round apparatus (Riko RH400-10W) unless otherwise stated.

Materials. Acetates **1a**—**1d** were obtained by acetylation with acetic anhydride in pyridine of the corresponding alcohols **3a**—**3d** which were prepared according to the literature.[12] Racemic and (*S*)-**1e** were obtained from commercially available (±)- and (*S*)-**3e**, respectively, by acetylation with acetic anhydride in CH_2Cl_2 in the presence of pyridine.

1-(9-Anthryl)ethyl Acetate (1a). Colorless plates; mp 101—102 °C (MeOH); IR 1740 ($\nu_{C=O}$) and 1250 cm^{-1}; ^{1}H NMR ($CDCl_3$) $\delta = 1.93$ (3H, d, $J = 7$ Hz, Me), 2.08 (3H, s, COMe), 7.4—7.6 (5H, m), 8.01 (2H, d, $J = 9$ Hz), 8.42 (1H, s, 9′-H), and 8.60 (2H, br d, 1′- and 8′-H).

1-(9-Anthryl)propyl Acetate (1b). Pale yellow plates; mp 85 °C (MeOH); IR 1740 ($\nu_{C=O}$) and 1245 cm^{-1}; ^{1}H NMR ($CDCl_3$) $\delta = 0.97$ (3H, t, $J = 7$ Hz, Me), 2.08 (3H, s, COMe), 2.3 (1H, m, CH_2), 2.5 (1H, m, CH_2), 7.21 (1H, t, $J = 7$ Hz, CH(OAc)), 7.4—7.6 (4H, m), 8.0 (2H, m), 8.42 (1H, s, 9′-H), and 8.62 (2H, br, 1′- and 8′-H).

1-(9-Anthryl)-2-methylpropyl Acetate (1c). Yellow plates; mp 143—144 °C (MeOH); IR 1730 ($\nu_{C=O}$) and 1240 cm^{-1}; ^{1}H NMR ($CDCl_3$, 400 MHz) $\delta = 0.56$ (3H, d, $J = 6.6$ Hz, Me), 1.28 (3H, d, $J = 6.6$ Hz, Me), 2.06 (3H, s, COMe), 2.92 (1H, m, C<u>H</u>Me$_2$), 6.93 (1H, d, $J = 10$ Hz, CH(OAc)), 7.4—7.6 (4H, m), 8.0 (2H, m), 8.41 (1H, s, 9′-H), 8.58 (1H, br), and 8.75 (1H, br).

1-(9-Anthryl)-2,2-dimethylpropyl Acetate (1d). Pale yellow plates; mp 185 °C (MeOH); IR 1730 ($\nu_{C=O}$) and 1250 cm^{-1}; ^{1}H NMR ($CDCl_3$) $\delta = 1.04$ (9H, s, Me×3), 2.14 (3H, s, COMe), 7.28 (1H, s, CH(OAc)), 7.35—7.56 (4H, m), 7.97 (2H, m), 8.41 (1H, s, 9′-H), 8.53 (1H, d, $J = 9$ Hz), and 8.88 (1H, m).

(±)-1-(9-Anthryl)-2,2,2-trifluoroethyl Acetate (±-1e). Colorless plates; mp 102 °C (MeOH); IR 1750 ($\nu_{C=O}$) and 1220 cm^{-1}; ^{1}H NMR ($CDCl_3$) $\delta = 2.21$ (3H, s, COMe), 7.4—7.7 (4H, m), 7.81 (1H, q, $^3J_{H-F} = 8$ Hz, C<u>H</u>CF$_3$), 8.03 (2H, d, $J = 8$ Hz), 8.36 (1H, m), 8.57 (1H, s, 9′-H), and 8.73 (1H, m).

(*S*)-1-(9-Anthryl)-2,2,2-trifluoroethyl Acetate ((*S*)-1e). Colorless fine crystals; mp 65—66 °C (MeOH).

Preparative Photolysis in Solution. A degassed benzene solution of **1a**—**1e** (0.025—0.03 M) was irradiated for 12 h. After the solvent was removed under reduced pressure, the residue was chromatographed on silica gel with benzene as eluent to give dimers as a colorless solid.

***meso*- and *dl*-Dimers of 1-(9-Anthryl)ethyl Acetate (2a).** IR 1732 ($\nu_{C=O}$), 1478, 1450, 1366, 1238, 1058, 778, and 688 cm^{-1}; ^{1}H NMR ($CDCl_3$) $\delta = 1.56$ (6H, d, $J = 6$ Hz, Me), 2.50 (6H, s, COMe), 4.20 (2H, s, 10,10′-H), 6.29, 6.30 (2H, each q, $J = 6$ Hz,

CH(OAc)), 6.8—7.0 (14H, m), and 7.5—7.6 (2H, m).

***meso*- and *dl*-Dimers of 1-(9-Anthryl)propyl Acetate (2b).** IR 1740 ($\nu_{C=O}$), 1480, 1455, 1365, 1230, 1100, 775, and 690 cm^{-1}; ^1H NMR ($CDCl_3$) δ = 1.06 (6H, t, J = 7.5 Hz, Me), 1.7 (2H, m, CH_2), 2.0 (2H, m, CH_2), 2.53 (6H, s, COMe), 4.15 (2H, s, 10, 10′-H), 6.35 (2H, d, J = 9 Hz, CH(OAc)), 6.75—7.0 (14H, m) and 7.6 (2H, m); ^{13}C NMR ($CDCl_3$) δ = 11.56 (Me), 22.02 ($CO\underline{C}H_3$), 25.21 (CH_2), 58.37 (*dl*) and 58.47 (*meso*) (C-10 and C-10′), 59.39 (*meso*) and 59.47 (*dl*) (C-9 and C-9′), 79.78 (*dl*) and 79.98 (*meso*) (CH(OAc)), and 171.76 (C=O).

***meso*-Dimer of 1-(9-Anthryl)-2-methylpropyl Acetate (*meso*-2c).** IR 1730 ($\nu_{C=O}$), 1480, 1455, 1385, 1365, 1230, 1015, 780, and 685 cm^{-1}; ^1H NMR ($CDCl_3$) δ = 0.43, 0.49, 1.02, 1.10, 1.33, 1.37, 1.87 (total 12H, each d, J = 7 Hz, Me), 1.81, 1.88, 2.52, 2.56 (total 6H, 2 : 1 : 4 : 2, each s, COMe), 2.3—2.7, 3.1—3.2 (total 2H, each m, $C\underline{H}Me_2$), 4.15, 4.16, 4.65, 4.68 (total 2H, 4 : 2 : 2 : 1, each s, 10,10′-H), 5.82, 5.97, 6.38, 6.46 (total 2H, 2 : 1 : 4 : 2, each d, J = 6 Hz, CH(OAc)), 6.7—7.1 (m), 7.54 (d, J = 8 Hz), and 7.80 (m).

(*S*,*S*)-1-(9-Anthryl)-2,2,2-trifluoroethyl Acetate Dimer ((*S*,*S*)-2e). IR 1765 ($\nu_{C=O}$), 1480, 1455, 1395, 1370, 1220, 1205, 1130, 1075, 1050, 950, 880, 860, 780, 755, and 690 cm^{-1}; ^1H NMR ($CDCl_3$) δ = 2.62 (6H, s, COMe), 4.17 (2H, s, 10,10′-H), 6.72 (2H, q, $^3J_{H-F}$ = 7 Hz, $C\underline{H}CF_3$), 6.8—7.0 (12H, m), 7.05 (2H, d, J = 7 Hz), and 7.41 (2H, m).

***meso*-1-(9-Anthryl)-2,2,2-trifluoroethyl Acetate Dimer (*meso*-2e).** IR 1765 ($\nu_{C=O}$), 1490, 1455, 1400, 1375, 1220, 1210, 1125, 1075, 1050, 960, 910, 880, 780, 745, and 690 cm^{-1}; The ^1H NMR spectrum is the same as (*S*,*S*)-**2e**.

Solid-State Photolysis. KBr disks containing the sample (2% w/w) were irradiated between two Pyrex® glass plates in a Pyrex® test tube under a vacuum. The progress of photodimerization was monitored with difference IR spectra. The photolytic mixture was extracted from the pellets with $CDCl_3$ and the dimer yields were calculated based on the integration ratio of ^1H NMR signals. As for large-scale experiments the powdered solid sample was placed between two glass plates in a polyethylene bag and irradiated under the same conditions. For monitoring of the X-ray powder pattern, a solid sample of **1b** (about 50 mg) was placed between two Pyrex® glass plates and irradiated at 20 °C. After irradiation the X-ray diffraction was recorded and at the same time a sample of the photolysate was dissolved in $CDCl_3$ and the ^1H NMR spectrum was measured to calculate the conversion. As for the single crystal experiment a crystal of **1b** (0.4×0.2×0.05 mm) whose quality was checked by peak profiles recorded on a Rigaku AFC-5R four-circle diffractometer was irradiated with a 100 W high-pressure mercury lamp through a Toshiba L-38 filter (> 380 nm). The appearance of the crystal was observed by a microscope.

Monitoring Photochemical Reactions by ^1H NMR Spectroscopy. A solution of **1a**—**1e** in C_6D_6 (about 0.03 M) was degassed and sealed in a Pyrex® NMR tube. The sample solution was irradiated at 25 °C and variations of ^1H NMR spectra were recorded after 3 and 6 h. To check thermal stability of the products, the photolysate was kept in the dark at room temperature for 3 h and the NMR spectrum was taken again.

Quantum Yield Measurements. Irradiation was done by a 100 W high-pressure mercury lamp through Toshiba UV-35 and UV-D1B filters. Photon flux was measured using $K_3[Fe(C_2O_4)]$ as actinometer. In the case of benzene solutions, each sample solution (2 cm^3) was irradiated in a 1-cm quartz cuvette with stirring under vacuum. The photolysate was evaporated, the residue was dissolved

Table 5. Crystal Data and Details for Structure Determination of **1a**—**1e**

Compound	**1a**	**1b**	**1c**	**1d**	**1e**
Crystal size/mm	0.5 × 0.3 × 0.2	0.5 × 0.4 × 0.1	0.5 × 0.3 × 0.2	0.5 × 0.3 × 0.1	0.4 × 0.2 × 0.05
Formula	$C_{18}H_{16}O_2$	$C_{19}H_{18}O_2$	$C_{20}H_{20}O_2$	$C_{21}H_{22}O_2$	$C_{18}H_{13}F_3O_2$
M_r	264.31	278.35	292.38	306.41	318.30
Crystal system	Orthorhombic	Triclinic	Monoclinic	Triclinic	Monoclinic
Space group	*Pbca*	$P\bar{1}$	$P2_1/n$	$P\bar{1}$	$P2_1/n$
a/Å	17.807(2)	10.292(2)	15.979(2)	10.965(3)	10.852(2)
b/Å	15.821(2)	10.784(2)	9.816(3)	11.233(4)	14.573(6)
c/Å	10.072(1)	8.469(1)	10.666(3)	9.017(2)	10.502(5)
α/°		100.70(1)		108.05(3)	
β/°		104.54(1)	108.81(1)	96.24(3)	113.08(4)
γ/°		116.06(1)		121.10(2)	
V/Å^3	2837.5(5)	768.6(3)	1583.7(6)	853.5(6)	1528(1)
Z	8	2	4	2	4
D_x/g cm^{-3}	1.237	1.203	1.226	1.192	1.383
λ/Å	1.54184	0.71068	1.54184	0.71068	0.71068
μ/cm^{-1}	5.95	0.77	5.34	0.75	1.14
Scan width/°	1.78+0.4tan θ	1.0+0.35tan θ	1.84+0.4tan θ	1.1+0.35tan θ	1.0+0.35tan θ
$2\theta_{max}$/°	120.0	50.0	120.0	55.0	50.0
No. of relections					
Measured		3480	2654	4177	2970
Observed	1789	2672	1968	2799	1341
Criterion for obsd	$I > 3\sigma(I)$	$F > 3\sigma(F)$	$F > 2\sigma(F)$	$F > 3\sigma(F)$	$I > 3\sigma(I)$
Absorption correction	ψ-scan	None	ψ-scan	None	None
Final R	0.039	0.062	0.042	0.049	0.054
R_w	0.035	0.059	0.046	0.043	0.037
No. of parameters	246	262	255	297	256
$(\Delta/\sigma)_{max}$	0.11	0.26	0.14	0.24	0.22
$\Delta\rho_{min}/\Delta\rho_{max}$	−0.13/0.13	−0.22/0.20	−0.17/0.15	−0.16/0.18	−0.19/0.15

into C_6D_6 or $CDCl_3$, and the dimer yield and stereoselectivity were calculated based on the integration ratio of ^{1}H NMR signals. As for the solid, a KBr pellet containing 2% w/w sample was irradiated with the same light source, and the pellet was powdered and extracted with $CDCl_3$. Irradiation was stopped at about 10% conversion. Each run was done two or three times.

X-Ray Structure Analysis of 1a—1e. A single crystal was mounted on a Rigaku AFC-5R or AFC-7R four-circle diffractometer. Intensity data were collected with Cu $K\alpha$ or Mo $K\alpha$ radiation using the 2θ–ω scan technique at about 295 K. Three standard reflections were monitored every 150 reflections and no significant variation in intensity was observed in either case. Crystal data and details of data collection were summarized in Table 5.[13] The structures were solved by direct methods by the program of SHELXS86[14] and refined by full-matrix least-squares methods on F with the weighting scheme of $[\sigma(F_o)^2+0.00018F_o^2]^{-1}$ using the program SHELX76[15] (for **1c**) or with the weight of $\sigma(F_o)^{-2}$ using the TEXSAN[16] system (for others). The methyl groups on **1c** and **1e** were treated as a rigid group while other H atoms were located on difference maps and refined isotropically.

Variable Temperature NMR Experiments. A sample solution of ca. 0.014 M acetates in CD_2Cl_2 (for **1a** and **1b**) or $CDCl_3$ (for **1c**—**1e**) was degassed in an NMR tube and sealed off. The ^{1}H NMR (400 MHz) spectra were recorded at various temperatures.

The authors wish to thank Professor Keiji Kobayashi, The University of Tokyo, for his help with measurements of solid-state fluorescence spectra. Thanks are also due to Professor Yutaka Fukuda, Ochanomizu University, for use of his spectrophotometer, and Professor Kayako Hori, Ochanomizu University, for her help with measurements of X-ray powder pattern. This work was supported by a Grant-in-Aid for Scientific Research No. 06740476 from Ministry of Education, Science and Culture.

References

1) M. D. Cohen and G. M. J. Schmidt, *J. Chem. Soc.*, **1964**, 1996.

2) D. P. Craig and P. Sarti-Fantoni, *J. Chem. Soc., Chem. Commun.*, **1966**, 742.

3) G. Kaupp, *Angew. Chem., Int. Ed. Engl.*, **31**, 595 (1992).

4) H. Bouas-Laurent, A. Castellan, and J.-P. Desvergne, *Pure Appl. Chem.*, **52**, 2633 (1980).

5) H. S. Rzepa, M. L. Webb, A. M. Z. Slawin, and D. J. Williams, *J. Chem. Soc., Chem. Commun.*, **1991**, 765.

6) H.-D. Becker and V. Langer, *J. Org. Chem.*, **58**, 4703 (1993).

7) A. Gavezzotti, in "Structure Correlation," ed by H.-B. Burgi and J. D. Dunitz, VCH, Weinheim (1994), p. 509.

8) a) M. Lahav, F. Laub, E. Gati, L. Leiserowitz, and Z. Ludmer, *J. Am. Chem. Soc.*, **98**, 1620 (1976); b) Z. Ludmer, M. Lahav, L. Leiserowitz, and L. Roitman, *J. Chem. Soc., Chem. Commun.*, **1982**, 326.

9) V. Enkelmann, G. Wegner, K. Novak, and B. Wagener, *J. Am. Chem. Soc.*, **115**, 10390 (1993).

10) G. M. J. Schmidt, *Pure Appl. Chem.*, **27**, 647 (1971).

11) F. C. De Schryver, L. Anand, G. Smets, and J. Switten, *Polym. Lett.*, **9**, 777 (1971).

12) I. de Riggi, A. Virgili, M. de Moragas, and C. Jaime, *J. Org. Chem.*, **60**, 27 (1995).

13) Lists of final positional and thermal parameters, bond distances and angles, and observed and calculated structure factors are deposited as Document No. 69031 at the Office of the Editor of Bull. Chem. Soc. Jpn.

14) G. M. Sheldrick, "SHELXS86. Program for Crystal Structure Determination," Univ. of Gottingen, Germany (1986).

15) G. M. Sheldrick, "SHELX76. Program for Crystal Structure Determination," Univ. of Cambridge, England (1976).

16) "TEXSAN: Crystal Structure Analysis Package," Molecular Science Corporation (1985).